POST-EVENT PLASTIC FAILURE ANALYSIS OF SHEAR FRAMES FROM THEIR PRE-EVENT ELASTIC RESPONSE

ARZHANG ALIMORADI, PH.D., P.E.

Abstract. We demonstrate that plastic failure loads of shear frames can be inferred from their elastic ambient response. The interstory plastic mechanism force is derived for moment-resisting (rigid) frames as a function of two measured elastic (low-amplitude) frequencies. Structural health monitoring techniques are traditionally devised for "post-event" assessment of structures after exposure of a facility to a potentially damaging loading event such as strong earthquakes or blasts. The knowledge of induced damage, its location, and severity in an otherwise functioning structure, as important as it is, may be too late for precautionary preparations. Naturally, one is interested in identification of potential failure mechanisms and indicators prior to damaging events when a structure is responding to environmental loads elastically. Are post-event plastic failure loads identifiable from the pre-event ambient response? We answer this question by first deriving interstory shear stiffness values from a set of measured ambient frequencies that are then incorporated into post-elastic equilibrium equations for a closed-form expression of failure loads as a function of measured frequencies. We test our procedure using a typical shear frame example as proof of concept.

To extend the relevance and applicability of the proposed procedure we consider uncertainties associated with the measured and estimated quantities and assess their effects in our model output. The closed-form solutions presented allow study of fully-stressed designs and we present the optimal stiffness distribution for such designs as another example.

It is anticipated that temporal relevance of structural health monitoring techniques to "pre-event" assessment will be extended in the near future to such promising technologies as earthquake early warning systems.

Contents

Date: 8/8/18.

2000 *Mathematics Subject Classification.* 70J10, 70J50, 74A10, 74C05, 74H10, 74H45.

Key words and phrases. Structural Health Monitoring, Plastic Failure Load, Shear Frames, Ambient Vibrations, Uncertainty Propagation, Fully-stressed Design.

Special thanks to Prof. James L. Beck for his comments and suggestions.

1. Introduction

Estimation of failure load probabilities in existing buildings in the context of structural health monitoring is difficult and expensive because of the scarcity of experimental data from structures at or near failure and difficulties with direct measurement of failure loads. We demonstrate analytically that plastic response of shear frames can be inferred from their experimental elastic response. Structural health monitoring (SHM) techniques are traditionally devised for "post-event" assessment of structures, after exposure of a facility to extreme and potentially damaging loading events such as strong earthquakes or blasts. Once exposure to a potentially damaging loading event is occurred, SHM is used to identify and locate the damage, its severity and reparability [1, 7, 14, 8, 9, 13, 10, 11, 48, 28, 29, 34, 25, 22, 16, 38]. More recently, the utility of SHM to "during-event" applications such as earthquake early warning systems has been proposed [49, 50, 51]. It is important to note that in the contemporary context of design for resiliency (exposure to multiple hazards) and design for sustainability (extended life cycle), continuous estimation of the state of a structure and its health is a necessary condition of operability. Are post-event plastic failure modes of a structure identifiable from its pre-event elastic response? Could inference be made, for example, on the location in a shear frame where failure would occur in the form of story plastic mechanism by observing the elastic vibration response of the frame? While condition assessment methods have been historically used to estimate the health of structural systems and their response, and to a lesser degree to identify the input loads for design and functionality purposes, the growing stock of aging infrastructure and frequent revisions to the provisions of building codes make answering these questions imperative.

Background. Two major impediments for implementation of system identification techniques in damage detection and condition assessment of structures have been historically viewed as problems of identifiability and uniqueness of solutions, and relevance of the identified modal properties to physical damage. These issues have attracted considerable research in recent years [1, 14, 7, 8, 9, 12, 18, 13, 10, 11, 48, 23, 28, 27, 29, 31, 34, 25, 22, 16, 38, 17, 40, 47, 37, 3, 4]. For example, in one of the most comprehensive studies performed to date on variation of natural frequencies in buildings it was found that heavy winds could decrease the fundamental frequencies by 2 to 4% while rainfalls would cause an increase in the frequencies by 3 to 5% for the building under investigation. The rain effects persisted for one to two weeks after which the frequencies returned to their pre-rain levels [20]. The formulation presented here eliminates the problems of identifiability and damage interpretation by avoiding numerical optimization in high-dimensional spaces using analytical structural dynamics and plastic analysis theories.

2. Formulation

The assessment of ultimate load bearing capacity of full-scale operating structures remains a major engineering challenge due to the complex physics involved, particularly in response of large nonlinear systems to dynamics loads, and because of variations in geometry, material properties, and loading conditions of constructed facilities [5, 15, 32, 30, 45]. Therefore, it is desirable to construct the ultimate load bearing capacity of major structural systems in closed-form, or provide a numerical procedure for its estimation, from observations of their ambient (low-amplitude) frequencies and following the commonly used and tested assumptions of structural analysis and dynamics.

The failure load capacity of a structure is affected by a large number of factors. The paper considers the well-established theories of plastic failure in shear frames [33, 36, 42] with a model that is simple and practical enough as deemed from practice and research of earthquake response of structures (e.g., soft-story phenomenon) [19]. We assume no information about structural members and their properties, instead, the proposed procedure relies only on a series of frequency measurements under ambient and operational loading conditions to produce estimates of failure load capacities at different locations. Such information may be used subsequently in condition assessment of the structure, its capacity to resist future loads, and to assist in strengthening design schemes.

Definition 1. The interstory failure load is defined as a shear force that creates a full plastic failure mechanism at the story under consideration.

Claim 2. The failure load at level i is:

$$p_{f_i} = \varepsilon_{y_i} \frac{H_i^2}{2d_i} \left(m^*_{i-1,1}\widehat{\omega}^2_{i-1,1}\right)^{\alpha} \left(m^*_{i,1}\widehat{\omega}^2_{i,1}\right) \left(m^*_{i-1,1}\widehat{\omega}^2_{i-1,1} - m^*_{i,1}\widehat{\omega}^2_{i,1}\right)^{\beta} \tag{2.1}$$

where $\alpha = \beta = 0$ if $i = 1$ and $\alpha = -\beta = 1$ otherwise. Note that $\frac{m^\star_{i-1,1}}{m^\star_{i,1}} > \left(\frac{\widehat{\omega}_{i,1}}{\widehat{\omega}_{i-1,1}}\right)^2$ is strictly required. In (2.1), $\varepsilon_y = \frac{F_y}{E}$ is the yield strain of the columns with the material yield stress, F_y , and the modulus of elasticity, E , H

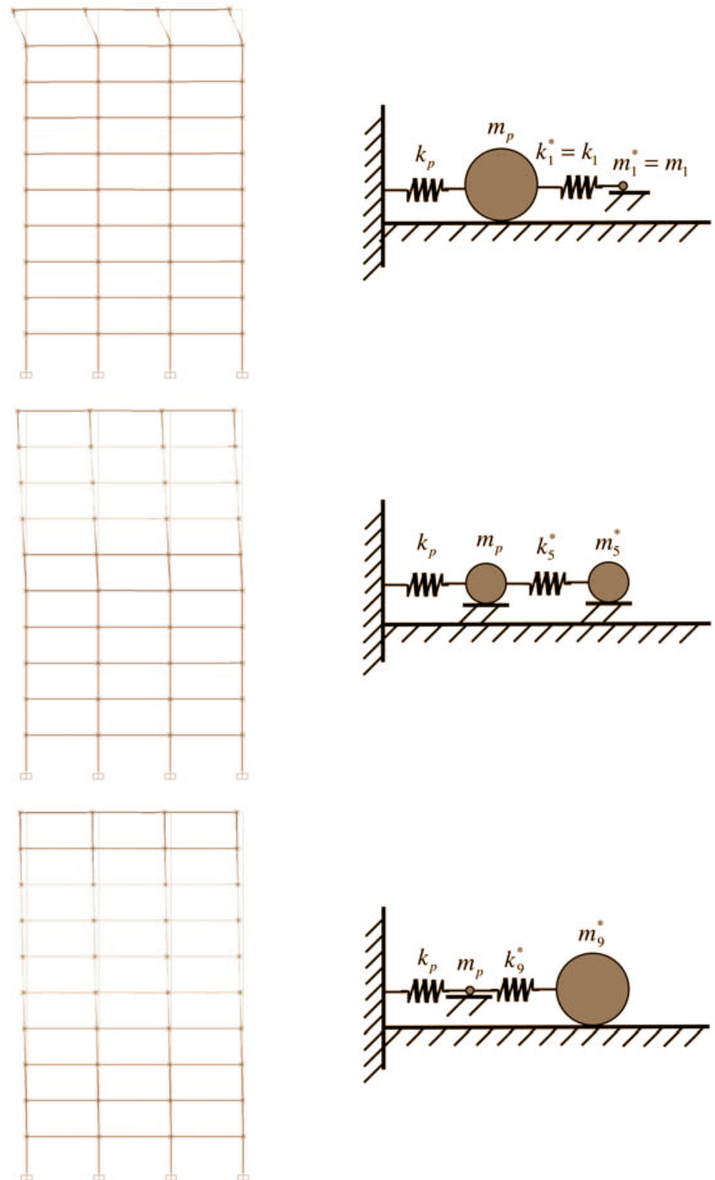

FIGURE 2.1. Examples of subsystems in a $10-dof$ shear frame (colors represent relative magnitude of displacements). The contact surfaces in mass-spring diagrams are frictionless and damping is assumed classical.

is the floor-to-floor height, and d is the depth of column sections within the floor[1]. The quotient in parentheses in (2.1) is the reciprocal of a hyperbolic paraboloid of modal frequencies and masses:

- $\widehat{\omega}_{i,1}$ is the measured fundamental frequency of subsystem i (as defined in §2.1 and 2.4),
- $m^*_{i,1} = \phi^T_{i,1}\mathbf{m}\phi_{i,1}$ is the fundamental modal mass of subsystem i with the mass matrix, $\mathbf{m}$, and the mode shape, $\phi_{i,1}$ (§2.2 describes its evaluation). The second subscript in the modal masses and frequencies is to emphasize that measurements are made in the fundamental mode of vibration, obtained easier and more reliable than other modes of vibration (more on this under §2.4).

Proof of (2.1) and illustrative examples follow.

2.1. **Lateral Stiffness.**

[1]One may argue that that ε_y, H, and d are unknown variables. The author claims that these quantities can be easily verified in the field. We assume that all column sections within each floor are of the same size.

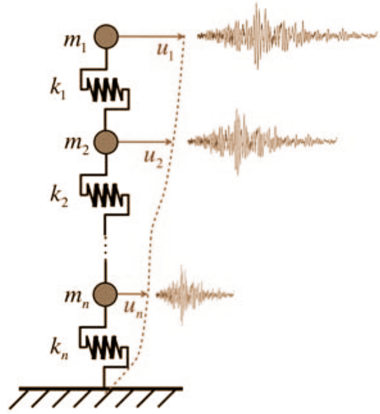

FIGURE 2.2. A schematic of the shear frame.

2.1.1. *Subsystems.* Consider the multi-story shear frame shown schematically in Figs. 2.1 and 2.2, idealized as an n-degree of freedom (NDOF) mass-spring system. We recursively derive the lateral stiffness of each degree of freedom, k_i, from a series of fundamental frequency analyses of the subsystems of the frame using one set of vibration measurements. Our analogy is akin to modeling of the generalized 2-degree of freedom systems such as those in tuned mass dampers [24] where a secondary oscillator is supported by a primary mass. The goal is to start with the lightest secondary system possible and successively transfer masses from the primary system to the secondary one, where floor levels occur, and estimate the modulus of springs connecting them (as in Fig. 2.1). For the rest of this paper, assume that subsystems are defined consecutively from the top floor of the frame to the bottom floor with each subsystem adding one degree of freedom to the previous subsystem. The identification of lateral stiffness is based frequency analyses of the subsystems, $\widehat{\omega}_{i,1} \in \mathbb{R}^+$, $i = 1, \ldots, n$, with the second subscript emphasizing the fundamental frequency of an i-mass subsystem and the overhat symbol indicating an uncertain measured quantity. With this definition, $\omega_{i,1}$ is the theoretical angular fundamental frequency of an i-mass subsystem.

If $n = 1$, $\omega_{1,1} = {}^{k_1}/_{m_1} \cong \widehat{\omega}^2_{1,1}$ where k_1 and m_1 are the stiffness and the mass of the top floor, respectively[2]. If $n \neq 1$, $\omega^2_{i,1} = {}^{k^*_{i,1}}/_{m^*_{i,1}} \cong \widehat{\omega}^2_{i,1}$ where the supported generalized mass on subsystem i is [21]:

$$m^*_{i,1} = \int_{x_1}^{x_i} \overline{m}(x)\psi_1^2(x)\,dx \tag{2.2}$$

$\overline{m}(x)$ and $\psi_1(x)$ are the distributed mass and the compatible shape function for the vibration of the i^{th} subsystem in its fundamental mode. For discrete shear frames with lumped masses at each floor level (2.2) becomes the fundamental modal mass of subsystem i, $m^*_{i,1} = \phi^T_{i,1}\mathbf{m}_i\phi_{i,1}$ where $\phi_{i,1} \in \mathbb{R}^{i\times 1}$ and $\mathbf{m}_i \in \mathbb{R}^{i\times i}$. Similarly, $k^*_{i,1}$ is the modal stiffness of subsystem i, $k^*_{i,1} = \phi^T_{i,1}\mathbf{k}_i\phi_{i,1}$.

Claim 3. The fundamental frequency of subsystem i is:

$$\omega^2_{i,1} = \frac{k^*_{i,1}}{m^*_{i,1}} = \frac{1}{m^*_{i,1}}\frac{\prod_{j=1}^{i} k_j}{\sum_{j=1}^{i}\left(\prod_{l=1,l\neq j}^{i} k_l\right)} \simeq \widehat{\omega}^2_{i,1} \qquad i = 1, \ldots, n \tag{2.3}$$

When the measured frequencies of subsystems, $\widehat{\omega}_{i,1}$'s, are available from a vibration monitoring scheme such as the procedure of §2.4, then (2.3) becomes a set of n nonlinear algebraic equations that can be solved for k_i, $i \in \{1, \ldots, n\}$ (shown in Appendix B) with the story stiffness values, k_i's, expressed as a hyperbolic paraboloid of the measured frequencies:

$$k_i = \left(m^*_{i-1,1}\widehat{\omega}^2_{i-1,1}\right)^{\alpha}\left(m^*_{i,1}\widehat{\omega}^2_{i,1}\right)\left(m^*_{i-1,1}\widehat{\omega}^2_{i-1,1} - m^*_{i,1}\widehat{\omega}^2_{i,1}\right)^{\beta} \tag{2.4}$$

where $\alpha = \beta = 0$ if $i = 1$ and $\alpha = -\beta = 1$ otherwise.

[2] k is the interstory stiffness, a scalar. k is a matrix that is composed of k's. The modal stiffness, also a scaler, is denoted by k^*.

Proof. By induction. See appendices A and B for the general case of an $n-$degree of freedom (NDOF) system. □

2.2. **Modal Mass.** The springs in Fig. 2.2 are in series, that is, their relative displacements are additive:

$$k_1\left(1-u_2\right)=k_2\left(u_2-u_3\right)=k_3\left(u_3-u_4\right)=\cdots=k_i u_i \tag{2.5}$$

or $u_j=1-k_i\left(\frac{1}{k_1}+\frac{1}{k_2}+\cdots+\frac{1}{k_{j-1}}\right)u_i$, hence from (2.2),

$$m_i^*=\sum_{j=1}^{i}\overline{m}_j\left[1-k_i\left(\frac{1}{k_1}+\frac{1}{k_2}+\cdots+\frac{1}{k_{j-1}}\right)u_i\right]^2,\qquad \text{where } u_1\equiv 1 \tag{2.6}$$

The estimation of $\overline{m}_j$ in (2.6) is possible using the guidelines of design codes and following the structure's design criteria. For our derivations we assume that $\overline{m}_j$'s are available and we study different methods estimating m_i^* in Appendix A. The quantification of uncertainties caused by the estimation of modal masses is presented in §3.

2.3. **Plastic Failure Load.** From equilibrium of forces at the onset of failure or the principle of virtual work [33, 26, 41], and with reference to Fig. 2.3, at any given level i the story mechanism shear force, $p_{f_i}=\sum_{j=1}^{i}p_j$, should satisfy:

$$\sum_{j=1}^{i}p_j H_i=2n_{c_i}M_{p_i},\qquad i=1,\ldots,n \tag{2.7}$$

where p_j's are the applied lateral loads at levels above level i, H_i is the height of the floor under consideration, n_{c_i} is the number of columns within the floor, and $M_{p_i}=F_{y_i}Z_i$ is the plastic moment capacity of prismatic columns with the material yield stress of F_{y_i} and the plastic section modulus of Z_i [41]. Note that the story shear force at failure is the sum of story forces from above. Eq. 2.7 can be rearranged as:

$$p_{f_i}=\sum_{j=1}^{i}p_j=\frac{\varsigma_i F_{y_i}}{d_i}\frac{k_i H_i^2}{6E_i}=C_{1,i}C_{2,i}H_i\frac{\left(m_{i-1,1}^*\widehat{\omega}_{i-1,1}^2\right)^{\alpha}m_{i,1}^*\widehat{\omega}_{i,1}^2}{\left(m_{i-1,1}^*\widehat{\omega}_{i-1,1}^2-m_{i,1}^*\widehat{\omega}_{i,1}^2\right)^{\beta}} \tag{2.8}$$

where k_i is the stiffness coefficient for floor i and the dimensionless constants C_1 and C_2 represent material and geometric scaling[3]:

$$C_{1,i}=\frac{F_{y_i}}{E_i}=\varepsilon_{y_i},\ C_{2,i}=\frac{\varsigma_i}{6}\frac{H_i}{d_i} \tag{2.9}$$

for the material modulus of elasticity, E_i and the columns section depth, d_i. $\varsigma_i=3$ for rectangular columns and $=2.3$ for I-shape columns. $k_i={}^{12n_{c_i}E_iI_i}/_{H_i^3}$ is the story shear stiffness with columns moment of inertia $I_i={}^{Z_id_i}/_{\varsigma_i}$ [41, 44].

Equation (2.8) can be used to arrive at the plastic failure shear force at any level of a multistory frame given two measured frequencies of its subsystems, one for the level above and one for the level under consideration.

2.4. **Experimental Scheme.** Our objective is to construct the full stiffness matrix of a shear frame from a series of fundamental frequency analyses of one set of ambient or micro-tremor vibration measurements of its subsystems, starting from the least restrained degree of freedom of the structure (usually the top floor) cumulatively adding one floor mass each time, to arrive at n dynamic equilibrium equations that can be solved recursively for the stiffness coefficients of system's stiffness matrix. With reference to Fig. 2.2, given the time series of relative acceleration at floor i with respect to base denoted as $\widehat{\ddot{u}}_i$, starting from $i=1$, we have:

- for $i=1$, $\left(\widehat{\ddot{u}}_1-\widehat{\ddot{u}}_2\right)\overset{FT}{\rightsquigarrow}\widehat{\omega}_{1,1}$, where FT denote a process of frequency transformation [35],
- for $i=2$, $\left(\widehat{\ddot{u}}_1-\widehat{\ddot{u}}_3\right)\overset{FT}{\rightsquigarrow}\widehat{\omega}_{2,1}$, *i.e.*, the fundamental frequency of the 2-mass subsystem,
- for $i=n$, $\widehat{\ddot{u}}_1\overset{FT}{\rightsquigarrow}\widehat{\omega}_{n,1}$, the fundamental angular frequency of the shear frames (the n-mass subsystem).

[3]As example of two common structural materials, for structural steel, $C_{1,\,\mathrm{steel}}={}^{50}/_{29000}=1.723\times10^{-3}$ and for normal-weight concrete with a 28-day compressive strength in the range of $f_c'=3000\rightarrow5000$ *psi*, $C_{1,\,\mathrm{concrete}}={}^{3000}/_{3140\times10^3}=9.554\times10^{-4}\rightarrow{}^{5000}/_{4050\times10^3}=1.230\times10^{-3}$.

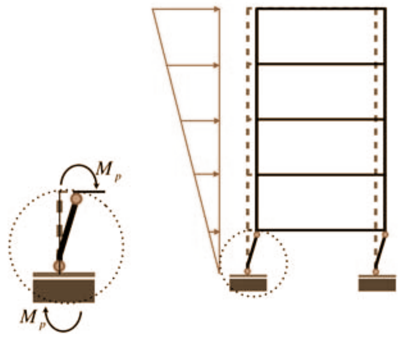

FIGURE 2.3. Equilibrium at the story plastic failure mechanism.

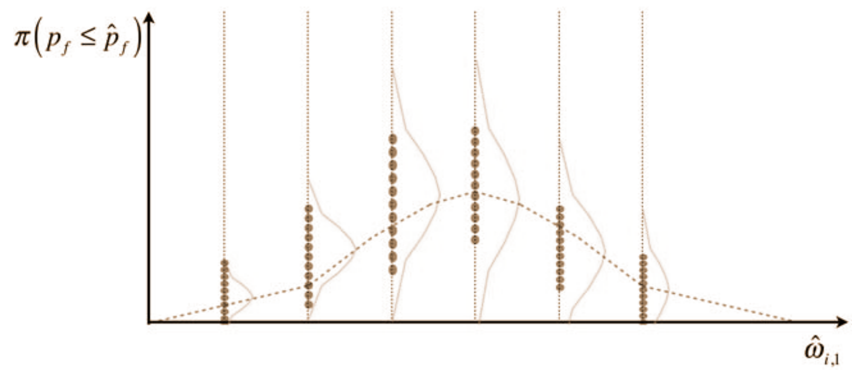

FIGURE 3.1. Schematic illustration of the Bayesian likelihood in one dimension (3.1). It is difficult and expensive to test structures with different frequencies to failure (grey dots).

With the angular frequencies and modal masses determined, the dynamic equilibrium equation (2.3) for subsystem i can be written:

$$\frac{\prod_{j=1}^{i} k_j}{\sum_{j=1}^{i}\left(\prod_{l=1,l\neq j}^{i} k_l\right)} = \omega_{i,1}^2 m_{i,1}^* \cong \widehat{\omega}_{i,1}^2 m_{i,1}^* \qquad i = 1,\ldots,n \tag{2.10}$$

Eq. (2.10) is a set of n nonlinear algebraic equations in measured frequencies of subsystems that can be solved for the interstory stiffness coefficients, k_j (Appendix B).

3. Analysis of Uncertainty

With dynamic response of nonlinear oscillators under stochastic excitations, the estimation of failure load probabilities, $\pi\left(p_{f_i} \leq \widehat{p_f}\right)$, is difficult and expensive because of the scarcity of experimental data from failure events and difficulties with the direct measurement of failure loads. Consequently, the application of updating methods for the probabilities of failure in existing structures, such as

$$\pi\left(p_{f_i} \leq \widehat{p_f}\,|\widehat{\omega}_{i-1,1}, \widehat{\omega}_{i,1}\right) = \frac{\pi\left(\widehat{\omega}_{i-1,1}, \widehat{\omega}_{i,1}\,|p_{f_i} \leq \widehat{p_f}\right)\pi\left(p_{f_i} \leq \widehat{p_f}\right)}{\int \pi\left(\widehat{\omega}_{i-1,1}, \widehat{\omega}_{i,1}\,|p_{f_i} \leq \widehat{p_f}\right)\pi\left(p_{f_i} \leq \widehat{p_f}\right) dp_{f_i}} \tag{3.1}$$

remains an open research enquiry chiefly due to the difficulties in the estimation of the likelihood term in (3.1), schematically illustrated in Fig. 3.1.

The model response in (2.8), obtained from structural dynamics and plastic failure theories, is a nonlinear parametrized model of four uncertain parameters:

(1) $m_{i-1,1}^* \sim \mathcal{N}\left(\mu_{m_{i-1,1}^*}, \sigma_{m_{i-1,1}^*}^2\right)$,
(2) $m_{i,1}^* \sim \mathcal{N}\left(\mu_{m_{i,1}^*}, \sigma_{m_{i,1}^*}^2\right)$,
(3) $\widehat{\omega}_{i-1,1}^2 \sim \mathcal{N}\left(\mu_{\widehat{\omega}_{i-1,1}^2}, \sigma_{\widehat{\omega}_{i-1,1}^2}^2\right)$, and

(4) $\widehat{\omega}_{i,1}^2 \sim \mathcal{N}\left(\mu_{\widehat{\omega}_{i,1}^2}, \sigma^2_{\widehat{\omega}_{i,1}^2}\right)$.

The first two uncertain parameters depend on the assumed mode shape and the mass matrix, and $\sigma^2_{\widehat{\omega}_{i,1}^2} \leq \sigma^2_{\widehat{\omega}_{i-1,1}^2}$. We now try quantifying the uncertainties associated with the predicted outcome of (2.8) due to the four aforementioned parameters [46]. The uncertainties are generally due to limited or incomplete data, the resolution of sensors, or our modeling assumptions in the treatment of underlying physical system.

3.1. **Assumptions.** Analytically, the only approximation made in the derivation of the equations is the parametrization of modal mass (*i.e.*, $\phi_{i,1}^T \mathbf{m}_i \phi_{i,1}$ is truncated, see §A.2). Practically, the methodology is limited by the following:

- 2D response and shear frames is assumed with lumped masses at each floor levels, the axial deformation of columns and 3D load redistribution effects on failure loads are ignored,
- The floor mechanism is assumed to be the controlling mechanism (shear-frame assumption),
- The upper-bound theorem of plasticity holds,
- Parametrized mode shapes are approximations since lateral deformations are assumed a function of lateral stiffness (Eq. 2.5), and
- Measurement errors, noise, and sensor dynamics.

These assumptions are normally accepted in the study and design practice of framed structures with regular mass and stiffness distribution. Building codes provide quantitative measures of regularity in this regard [6].

Remark. With the sequence of assessments defined by the subsystems uncertainties associated with estimates of failure loads reduce as the procedure continues from top to bottom of a frame, thanks to availability of more sensor data for lower levels that make more accurate estimates of frequencies possible. This is an advantage since the lower levels of frames carry larger gravity loads compared to the top levels and their failure can be more catastrophic.

3.2. **Uncertain Frequencies.** The probability distribution of interstory mechanism shear force is modeled as [46]:

$$p_{f_{i,j}} = f\left(\Theta_{i,j}\right) + \varepsilon_j, \quad j = 1, \cdots, l \tag{3.2}$$

for l observations with ε_j's as independent and identically distributed (iid) variables and $\Theta_i \sim \mathcal{N}\left(\mu_{\Theta_i}, \sigma^2_{\Theta_i}\right)$, where the vector of uncertain parameters is $\Theta_i = \left\{\widehat{\omega}_{i-1,1}, \widehat{\omega}_{i,1}\right\}^T$. Applying the perturbation method to (3.2) the propagation of uncertainties to model output can be estimated using a truncated multidimensional Taylor expansion around the expected values of the uncertain parameters $\Theta_i = \mu_{\Theta_i} + \delta\Theta_i = \left\{\mu_{\widehat{\omega}_{i-1,1}} + \delta\widehat{\omega}_{i-1,1}, \mu_{\widehat{\omega}_{i,1}} + \delta\widehat{\omega}_{i,1}\right\}^T$:

$$\begin{aligned} p_{f_i} &\cong f\left(\mu_{\Theta_i}\right) + \sum_{k=1}^{2} \left.\frac{\partial f}{\partial \Theta_{i,k}}\right|_{\mu_{\Theta_i}} \delta\Theta_{i,k} + \frac{1}{2}\sum_{l,k=1}^{2} \left.\frac{\partial^2 f}{\partial \Theta_{i,k}\partial\Theta_{i,l}}\right|_{\mu_{\Theta_i}} \delta\Theta_{i,k}\delta\Theta_{i,l} \\ &\simeq \mu_{p_{f_i}} + \sum_{k=1}^{2} s_{i,k}\delta\Theta_{i,k} \end{aligned} \tag{3.3}$$

for a first-order approximation of the failure load distribution. $s_{i,k}$ is the sensitivity of failure load to measured frequencies:

$$s_{i,1} = \left.\frac{\partial p_{f_i}}{\partial \widehat{\omega}_{i-1,1}}\right|_{\mu_{\Theta_i}} = -2C_{1,i}C_{2,i}H_i \frac{m^*_{i-1,1}\mu_{\widehat{\omega}_{i-1,1}} {m^*_{i,1}}^2 \mu^4_{\widehat{\omega}_{i,1}}}{\left(m^*_{i-1,1}\mu^2_{\widehat{\omega}_{i-1,1}} - m^*_{i,1}\mu^2_{\widehat{\omega}_{i,1}}\right)^2} \tag{3.4}$$

and

$$s_{i,2} = \left.\frac{\partial p_{f_i}}{\partial \widehat{\omega}_{i,1}}\right|_{\mu_{\Theta_i}} = -2C_{1,i}C_{2,i}H_i \frac{{m^*_{i-1,1}}^2\mu^4_{\widehat{\omega}_{i-1,1}} m^*_{i,1} \mu_{\widehat{\omega}_{i,1}}}{\left(m^*_{i-1,1}\mu^2_{\widehat{\omega}_{i-1,1}} - m^*_{i,1}\mu^2_{\widehat{\omega}_{i,1}}\right)^2} \tag{3.5}$$

Hence

$$p_{f_i}\left(\widehat{\omega}_{i-1,1}, \widehat{\omega}_{i,1}\right) \sim \mathcal{N}\left(\bar{y}_i, \mathbf{s}_i^T V_i \mathbf{s}_i\right) \tag{3.6}$$

where

$$E\left(p_{f_i}\right) = \bar{y}_i = f\left(\mu_{\Theta_i}\right) \tag{3.7}$$

and

$$\operatorname{var}\left(p_{f_i}\right) = \mathbf{s}_i^T V_i \mathbf{s}_i,\ V_i = \operatorname{diag}\left(\sigma^2_{\widehat{\omega}_{i-1,1}}, \sigma^2_{\widehat{\omega}_{i,1}}\right),\ \mathbf{s}_i^T = \{s_{i,1}, s_{i,2}\} \tag{3.8}$$

3.3. **Uncertain Modal Masses.** Assuming modal masses as uncertain

$$y = p_{f_{i,j}} = f\left(m^*_{i-1,1}, m^*_{i,1}\right) + \varepsilon_j, \quad j = 1, \cdots, l \tag{3.9}$$

where the vector of uncertain parameters for a given realization of modal masses is

$$\Theta_i = \mu_{\Theta_i} + \delta\Theta_i = \left\{\mu_{m^*_{i-1,1}} + \delta m^*_{i-1,1}, \mu_{m^*_{i,1}} + \delta m^*_{i,1}\right\}^T \tag{3.10}$$

the Taylor expansion of response about the mean value of uncertain parameters, as in (3.3) gives

$$p_{f_i} \simeq \mu_{p_{f_i}} + \sum_{k=1}^{2} s_{i,k}\delta\Theta_{i,k} \tag{3.11}$$

where the sensitivity of failure loads to modal masses is presented by a first-order approximation [46]:

$$s_{i,1} = \left.\frac{\partial p_{f_i}}{\partial m^*_{i-1,1}}\right|_{\mu_{\Theta_i}} = -C_{1,i}C_{2,i}H_i \frac{\mu^2_{m^*_{i,1}}\widehat{\omega}^4_{i,1}\widehat{\omega}^2_{i-1,1}}{\left(\mu_{m^*_{i-1,1}}\widehat{\omega}^2_{i-1,1} - \mu_{m^*_{i,1}}\widehat{\omega}^2_{i,1}\right)^2} \tag{3.12}$$

and

$$s_{2,1} = \left.\frac{\partial p_{f_i}}{\partial m^*_{i,1}}\right|_{\mu_{\Theta_i}} = C_{1,i}C_{2,i}H_i \frac{\mu^2_{m^*_{i-1,1}}\widehat{\omega}^2_{i,1}\widehat{\omega}^4_{i-1,1}}{\left(\mu_{m^*_{i-1,1}}\widehat{\omega}^2_{i-1,1} - \mu_{m^*_{i,1}}\widehat{\omega}^2_{i,1}\right)^2} \tag{3.13}$$

The expected value of response is estimated at the mean value of modal masses, *i.e.*

$$E\left(p_{f_i}\right) = \bar{y}_i = f\left(\mu_{m^*_{i-1,1}}, \mu_{m^*_{i,1}}\right) \tag{3.14}$$

and its variance is

$$\operatorname{var}\left(p_{f_i}\right) = \mathbf{s}_i^T V_i \mathbf{s}_i,\ V_i = \operatorname{diag}\left(\sigma^2_{m^*_{i-1,1}}, \sigma^2_{m^*_{i,1}}\right),\ \mathbf{s}_i^T = \{s_{i,1}, s_{i,2}\} \tag{3.15}$$

4. Illustrative Examples

4.1. **Verification with Theoretical Results.** The first example is a 3-bay 10-story shear frame shown in Fig. 4.1, analyzed and designed per provisions of American standards of practice [2, 6]. The bay widths are $L = 24.0$ feet each and the story heights are $H = 12.0$ feet at each level. A finite element model of the frame with a hundred beam-column members was analyzed under self weight and distributed live load of $3.0\,{}^{kip}\!/_{ft}$ on each beam. All girders are of American wide flange section size $W18 \times 192$. The first four story column sections are $W12 \times 120$, the column sections for levels five to eight are $W12 \times 72$ and the top two level columns are of $W12 \times 35$ section. The peak live load deformation was observed to be -1.03" $< {}^{L}\!/_{360}$ (Fig. 4.1 middle panel - note: color coding is only to show the relative magnitude of deformations). The frame was also subject to seismic loads following IBC 2012 equivalent lateral load provisions with a response modification factor of $R = 6$, the over-strength ratio of $\Omega = 3$, the displacement amplification factor of $C_d = 4$ at a site class C location with the scaled short duration spectral acceleration of $S_s = 2.29$ and the a scaled 1-second spectral acceleration of $S_1 = 0.869$ resulting in a base shear coefficient of $C_s = 0.132$. The peak lateral deformation (4.1 right panel) resulted under the $V = 80.37\,kip$ base shear is 3.40" equivalent to 0.24% of total frame height. The top three natural periods of the frame were observed to be $T_1 = 1.18$ sec (accounting for 78% of the modal participating mass laterally), $T_2 = 0.436$ sec (90% cumulative modal participating mass), and $T_3 = 0.271$ sec (95% cumulative modal participating mass).

FIGURE 4.1. Example 1 and its gravitational (middle panel) and lateral defections (right panel).

TABLE 1. Interstory Stiffness Values Obtained for Example 1.

Story, i	Elevation, in	Z_i, in^3	$C_{1,i}$	$C_{2,i}$	$\widehat{\omega}_i$, $^{rad}/_{sec}$	m_i, $^{k\cdot s^2}/_{in}$	m_i^* (Approximate)	k_i, $^{kip}/_{in}$
1	1440	51	0.00170	4.414	28.286	0.1496	0.157	132.019
2	1296	51	0.00170	4.414	17.447	0.1520	0.197	130.971
3	1152	108	0.00170	4.486	14.599	0.1544	0.245	272.392
4	1008	108	0.00170	4.486	12.354	0.1564	0.295	272.210
5	864	108	0.00170	4.486	10.568	0.1564	0.346	272.993
6	720	108	0.00170	4.486	9.160	0.1564	0.397	270.849
7	576	186	0.00170	4.212	8.505	0.1596	0.449	501.023
8	432	186	0.00170	4.212	7.917	0.1624	0.501	498.747
9	288	186	0.00170	4.212	7.383	0.1624	0.553	501.488
10	144	186	0.00170	4.212	6.848	0.1624	0.605	500.635

TABLE 2. Failure Loads in Example 1.

p_{f_i} (m_i^* Approximate), kip	p_{f_i} (m_i^* Exact), kip	p_{f_i} (Theoretical), kip
129.338	142.652	142.222
123.226	141.520	142.222
444.953	299.134	300.000
360.987	298.934	300.000
300.105	299.794	300.000
267.429	297.439	300.000
1313.205	516.604	516.667
971.582	514.256	516.667
779.275	517.084	516.667
498.484	516.203	516.667

Applying the procedure of §2, one obtains the interstory stiffness coefficients at different levels of the frame (see Table 1). For comparison with theoretical results we take $\widehat{\omega}_i = \omega_i$. The subsystem angular frequencies are from the finite element model by restraining the floor levels synthetically as in Fig. 2.1. Calculation of modal masses in Table 1, even with the constant stiffness approximation (Eq. A.17), correctly identifies the critical levels of the frame where columns are near their full capacity (*i.e.*, stress demand to capacity ratio of 1.0 from AISC 360-10 PMM Equation H1-1a) as in the finite element model (Fig. 4.3). With a better modal mass approximation the failure loads identified are nearly identical to the theoretical values (Table 2 and Fig. 4.2).

The identified interstory shear failure loads appear to be sensitive to the value of modal mass (Fig. 4.2) between floor levels where change in the column section occurs.

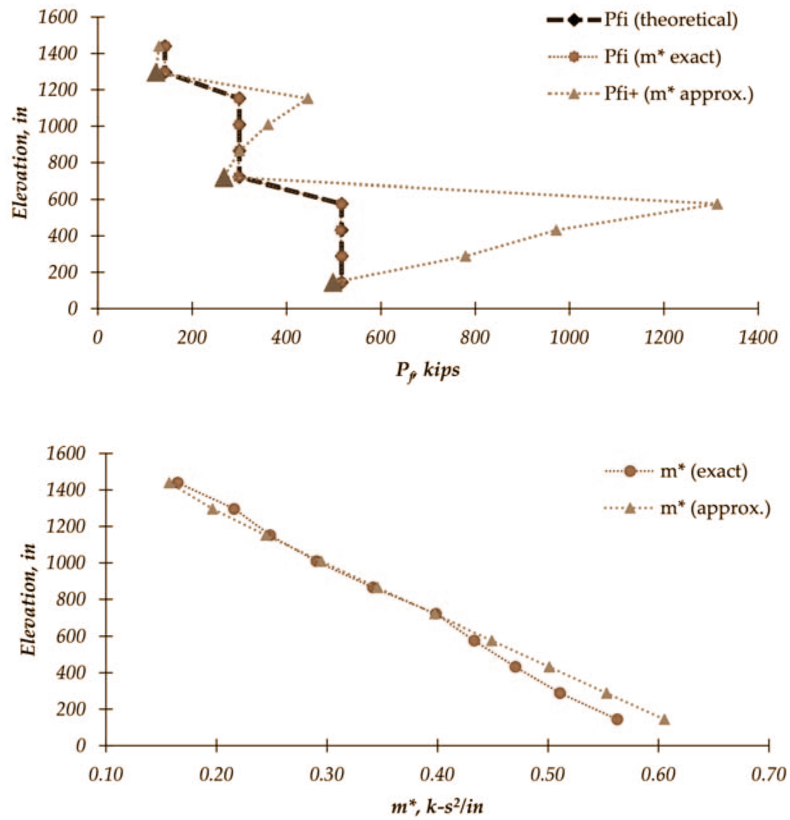

FIGURE 4.2. Story plastic failure loads from frequency analysis in Example 1.

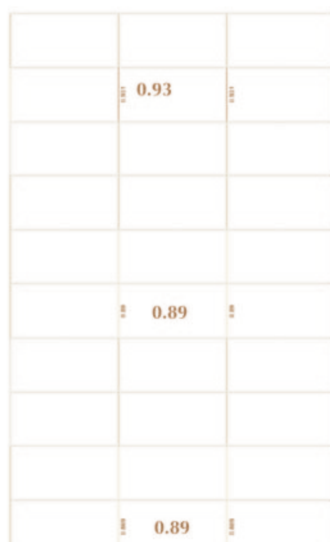

FIGURE 4.3. Demand-to-capacity ratios (strength utilization) for stories in Example 1. Levels with values above 85% are highlighted.

4.2. **Stiffness Distribution for Fully-stressed Designs.** Motivated by the idea of optimal material distribution for full utilization (*i.e.*, members stress demand to capacity ratio of 1.0) under design loads [43, 39], we define a *fully-stressed design* in the context of failure in shear frames as a stable arrangement of structural members such that the resulting frame fails simultaneously at all stories under the application of design loads. For a shear frame loaded laterally as in Fig. 4.4, where the profile of the applied loads follows the common static load equivalent approximation of dynamic codes in modern building codes (such as [6]), the top floor plastic mechanism failure force is available from (2.8):

$$C_1 C_2 H_1 k_1 = C_s W \frac{m_1 \sum_{i=1}^n H_i}{\sum_{i=1}^n m_i \sum_{j=i}^n H_j} \tag{4.1}$$

where $C_{1,i} = C_1$ and $C_{2,i} = C_2\,\forall i$. C_s is the seismic coefficient (or base-shear coefficient) expressed as a percentage of the building's total weight, W, that needs to be distributed and applied laterally to design the members of the frame for stressed and deformations induced during the course of lateral response. Such approximation is based on the assumption of dominant first-mode of vibration response, generally acceptable for frame structures without abrupt changes in their stiffness and mass. Eq. (4.1) can be rearranged for the value of interstory stiffness as

$$k_1 = \Gamma W \frac{m_1 \sum_{i=1}^n H_i}{H_1} \tag{4.2}$$

where

$$\Gamma \equiv \frac{C_s}{C_1 C_2} \frac{1}{\sum_{i=1}^n m_i \sum_{j=i}^n H_j} \propto \left[\frac{1}{\text{Mass}\times\text{Length}}\right] \tag{4.3}$$

For the story immediately below the top floor, from equilibrium of forces we have

$$C_1 C_2 \left(H_2 k_2 - H_1 k_1\right) = C_s W \frac{m_2 \sum_{i=2}^n H_i}{\sum_{i=1}^n m_i \sum_{j=i}^n H_j} \tag{4.4}$$

that simplifies to

$$k_2 = \frac{1}{H_2} \Gamma W \left(m_1 \sum_{i=1}^n H_i + m_2 \sum_{i=2}^n H_i \right) \tag{4.5}$$

Repeating the procedure iteratively one obtains a general expression for the optimal stiffness distribution of interstory stiffness values in the fully-stressed state under the assumption made hitherto. For an arbitrary story level i

$$k_i = \frac{1}{H_i} \Gamma W \sum_{j=1}^i m_j \sum_{l=j}^n H_l \tag{4.6}$$

Corollary. *For* $m_i = m$, $\forall i$

$$\begin{aligned} k_i &= \frac{1}{H_i} \mathit{\Gamma} W \left[m\left(H_1 + H_2 + \cdots + H_n\right) + m\left(H_2 + H_3 + \cdots + H_n\right) + \cdots + m\left(H_i + H_{i+1} + \cdots + H_n\right)\right] \\ &= \frac{m}{H_i} \mathit{\Gamma} W \left(\sum_{j=1}^i j \cdot H_j + \sum_{j=i+1}^n i \cdot H_j \right) \end{aligned} \tag{4.7}$$

Furthermore, if $H_i = H$, $\forall i$

$$k_1 = \frac{m}{H} \mathit{\Gamma} W \left(nH\right) = nm\mathit{\Gamma} W$$

$$k_2 = \frac{m}{H} \mathit{\Gamma} W \left(nH + \left(n-1\right)H\right) = \left(2n-1\right) m \mathit{\Gamma} W$$

$$k_3 = \frac{m}{H} \mathit{\Gamma} W \left(nH + \left(n-1\right)H + \left(n-2\right)H\right) = \left(3n-3\right) m \mathit{\Gamma} W$$

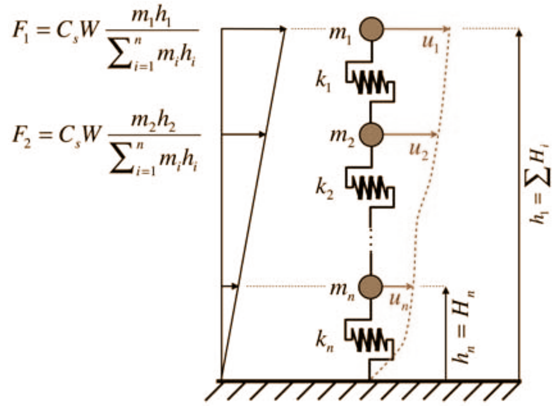

FIGURE 4.4. Fully-stressed design in the context of equivalent lateral load analysis.

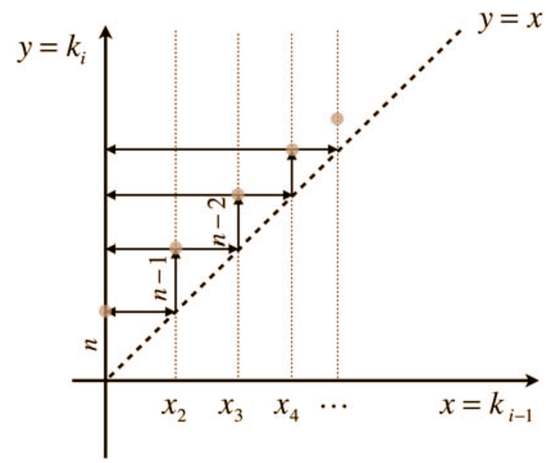

FIGURE 4.5. A linear map of fully-stressed stiffness values.

$$\vdots$$

$$k_i = k_{i-1} + (n - i + 1) \tag{4.8}$$

when $\Gamma W m$ is scaled to 1. Eq. (4.8) is a linear non-homogenous recurrence relationship of first-order, shown graphically in Fig. 4.5 converging to $k_{n-1} + 1$ as $i \to n$. Interestingly under the assumed conditions, common in most engineered moment frames, this implies larger changes in interstory shear stiffness of higher levels of tall frames (large n and small i) to meet the objective of fully-stressed design.

5. Concluding Remarks

A procedure for identification of interstory shear failure forces in moment-resisting frames was presented. It was shown that the failure forces can be expressed as a function of successive modal masses and frequencies in a series of subsystems whose frequencies are obtained experimentally and their modal masses are available analytically. The important issue of uncertainties in the estimates of natural frequencies and modal masses, while manageable by the methods of high-dimensional simulation such as Markov Chain Monte Carlo (MCMC), was shown to be analytically tractable by the perturbation of uncertain variables around their mean values. An example provided comparison of the shear failure forces obtained from the presented procedure with the theoretical results from plastic failure analysis in a ten story moment-resisting frame. The analytical expressions of plastic shear failure force allow their consideration in design and as another example this was shown in the problem of fully-stressed design of frames. It is hoped that the application of similar techniques in "pre-event" assessment of structures will be considered in such promising technologies as earthquake early warning systems for "during- and post-event" decision-making and analysis.

Future Research Directions. Continues monitoring of critical infrastructure for functionality and safety is an evolving area of research and the ability to incorporate probabilistic estimates of future performance an essential part of managing their risk. The presented procedure is a proof-of-concept in performance assessment of a particular yet common type of structures under extreme loading from their operational conditions. Extension to and developments for other types of structures and configurations as well as extensive computational and experimental verification under different loading histories and structural conditions are anticipated and outside the scope of this paper. Such enhancements should include consideration of 3-dimensional effects in the response of structure and a more detailed dynamic collapse capacity assessment for transient and high-rate loading scenarios which, by itself, is an important research undertaking.

References

[1] M. S. Agbabian, S. F. Masri, R. K. Miller, and T. K. Caughey. System identification approach to detection of structural changes. *Journal of Engineering Mechanics*, 117(2):370 – 390, 1991.

[2] AISC. *Steel Construction Manual*. American Institute of Steel Construction, 14th edition.

[3] Arzhang Alimoradi, Eduardo Miranda, Shahram Taghavi, and F. Naeim. Evolutionary modal identification utilizing coupled shear-flexural response - implication for multistory buildings. part i: Theory. *Structural Design of Tall and Special Buildings*, 15:51–65, 2006.

[4] Arzhang Alimoradi and F. Naeim. Evolutionary modal identification utilizing coupled shear-flexural response - implication for multistory buildings. part ii: Application. *Structural Design of Tall and Special Buildings*, 15:67–103, 2006.

[5] Y. Araki and K. D. Hjelmstad. Criteria for assessing dynamic collapse of elastoplastic structural systems. *Earthquake Engineering and Structural Dynamics*, 29(8):1177–1198, 2000.

[6] ASCE. *ASCE/SEI 7-10 Minimum Design Loads for Buildings and Other Structures*. American Society of Civil Engineers, 2010.

[7] J. L. Beck and L. S. Katafygiotis. Probabilistic system identification and health monitoring of structures. In *Proceedings of the Tenth World Conference on Earthquake Engineering*, pages 3721–3726, Madrid, Spain, July 1992.

[8] J. L. Beck, B. S. May, and D. C. Polidori. Determination of modal parameters from ambient vibration data for structural health monitoring. In *Proceedings of the First World Conference on Structural Control*, pages TA3–3–TA3–12, Los Angeles, CA, 1994. International Association for Structural Control.

[9] J. L. Beck, M. W. Vanik, and L. S. Katafygiotis. Determination of stiffness changes from modal parameter changes for structural health monitoring. In *Proceedings of the First World Conference on Structural Control*, pages TA3–13–TA3–22, Los Angeles, CA, 1994. International Association for Structural Control.

[10] James L. Beck. *Determining Models of Structures From Earthquake Records*. PhD thesis, California Institute of Technology, 1978.

[11] James L. Beck. Bayesian system identification based on probability logic. *Structural Control and Health Monitoring*, 17(7):825–847, 2010.

[12] James L. Beck and Siu-Kui Au. Bayesian updating of structural models and reliability using markov chain monte carlo simulation. *Journal of Engineering Mechanics*, 128(4):380–391, 2002.

[13] James L. Beck and L. S. Katafygiotis. Updating models and their uncertainties. part i: Bayesian statistical framework. *Journal of Engineering Mechanics*, 124(4):455–461, 1998.

[14] J.L. Beck. Bayesian system identification and response predictions robust to modeling uncertainty. ICOSSAR 2013, June 2013.

[15] V. R. M. Challa and J. F. Hall. Earthquake collapse analysis of steel frames. *Earthquake Engineering and Structural Dynamics*, 23(11):1199–1218, 1994.

[16] A. G. Chassiakos, S. F. Masri, A. Smyth, and J. C. Anderson. Adaptive methods for identification of hysteretic structures. In *Proceedings of the 1995 American Control Conference*, volume 3, pages 2349–2353, Seattle, WA, 1995.

[17] Anastassios G. Chassiakos and Sami F. Masri. Identification of structural systems by neural networks. *Mathematics and Computers in Simulation*, 40(5):637–656, 1996.

[18] Sai Hung Cheung and James L. Beck. Bayesian model updating using hybrid monte carlo simulation with application to structural dynamic models with many uncertain parameters. *Journal of Engineering Mechanics*, 135(4):243–255, 2009.

[19] Anil K. Chopra. *Dynamics of Structures*. Series in Civil Engineering and Engineering Mechanics. Prentice Hall International, 2011.

[20] John F. Clinton, S. Case Bradford, Thomas H. Heaton, and Javier Favela. The observed wander of the natural frequencies in a structure. *Bulletin of the Seismological Society of America*, 96(1):237–257, 2006.

[21] R.W. Clough and J. Penzien. *Dynamics of Structures*. McGraw-Hill, 1975.

[22] S. W. Doebling, C. R. Farrar, M. B. Prime, and D. W. Shevitz. Damage identification and health monitoring of structural and mechanical systems from changes in their vibration characteristics: A literature review. Technical report, Los Alamos National Laboratory, 1996.

[23] J. Ghaboussi and M. R. Banan. Neural networks in engineering diagnostics. Technical Report No. 941116, SAE, 1994.

[24] J. P. Den Hartog and J. Ormondroyd. Theory of the dynamic vibration absorber. *ASME J. Appl. Mech*, 50(7):11–22, 1928.

[25] K.D. Hjelmstad. On the uniqueness of modal parameter estimation. *Journal of Sound and Vibration*, 192(2):581–598, 1996.

[26] K.D. Hjelmstad. *Fundamentals of Structural Mechanics*. Springer, 2005.

[27] K.D. Hjelmstad, M. R. Banan, and M. R. Banan. On building finite element models of structures from modal response. *Earthquake Engineering and Structural Dynamics*, 24(1):53–67, 1995.

[28] Keith D. Hjelmstad and Soobong Shin. Damage detection and assessment of structures from static response. *Journal of Engineering Mechanics*, 123(6):568–576, 1997.

[29] G. W. Housner, L. A. Bergman, T. K. Caughey, A. G. Chassiakos, R. O. Claus, S. F. Masri, R. E. Skelton, T. T. Soong, B. F. Spencer, and J. T. P. Yao. Structural control: Past, present, and future. *Journal of Engineering Mechanics*, 123(9):897–971, 1997.

[30] L. F. Ibarra and H. Krawinkler. Global collapse of deteriorating mdof systems. In *13th World Conference on Earthquake Engineering*, 2004.

[31] W.D. Iwan. Extreme event performance evaluation using real-time hysteresis monitoring. In *International Workshop on Advanced Sensors, Structural Health Monitoring and Smart Structures*, Keio University, Japan, 2003.

[32] P. C. Jennings and R. Husid. Collapse of yielding structures during earthquakes. *Journal of Engineering Mechanics*, 94(EM5):1045–1065, 1968.

[33] Milan Jirasek and Zdenek P. Bazant. *Inelastic Analysis of Structures*. Wiley, 1st edition edition, 2001.

[34] L.S. Katafygiotis and J.L. Beck. Updating models and their uncertainties. part ii: Model identifiability. *Journal of Engineering Mechanics*, 124(4):463–467, 1998.

[35] Erwin Kreyszig. *Advanced Engineering Mathematics*. Wiley, 2011.

[36] Jacob Lubliner. *Plasticity Theory*. Dover Books on Engineering, 2008.

[37] P. Z. Marmarelis and F. E. Udwadia. The identification of building structural systems ii. the nonlinear case. *Bulletin of the Seismological Society of America*, 66(1):153–171, 1976.

[38] S. F. Masri, A. G. Chassiakos, and T. K. Caughey. Identification of nonlinear dynamic systems using neural networks. *Journal of Applied Mechanics*, 60(1):123–133, 1993.

[39] Keith Mueller, Min Liu, and Scott A. Burns. Fully stressed design of frame structures and multiple load paths. *Journal of Structural Engineering*, 128(6):806–814, 2002.

[40] C. Papadimitriou, J. L. Beck, and L. S. Katafygiotis. Asymptotic expansions for reliabilities and moments of uncertain dynamic systems. *Journal of Engineering Mechanics*, 123(12):1219–1229, 1997.

[41] Egor Popov. *Engineering Mechanics of Solids*. Prentice Hall, second edition edition, 1999.

[42] William Prager. Recent developments in the mathematical theory of plasticity. *AIP Journal of Applied Physics*, 20(3):235–241, 1949.

[43] Reza Razani. Behavior of fully stressed design of structures and its relationship to minimum-weight design. *AIAA Journal*, 3(12):2262–2268, 1965.

[44] C.G. Salmon, J.E. Johnson, and F.A. Malhas. *Steel Structures: Design and Behavior*. Prentice Hall, 2008.

[45] M. V. Sivaselvan and A. M. Reinhorn. Nonlinear structural analysis towards collapse simulation -a dynamical systems approach. Technical report, MCEER, University at Buffalo, 2003.

[46] Ralph C. Smith. *Uncertainty Quantification Theory, Implementation, and Applications*. Computational Science and Engineering. SIAM, 2014.

[47] Firdaus E. Udwadia and Panos Z. Marmarelis. The identification of building structural systems i. the linear case. *Bulletin of the Seismological Society of America*, 66(1):125–151, 1976.

[48] Michael W. Vanik, J. L. Beck, and Siu-Kui Au. Bayesian probabilistic approach to structural health monitoring. *Journal of Engineering Mechanics*, 126(7):738–745, 2000.

[49] Stephen Wu and James L. Beck. Synergistic combination of systems for structural health monitoring and earthquake early warning for structural health prognosis and diagnosis. volume 8348, pages 83481Z–83481Z–10, 2012.

[50] Stephen Wu, James L Beck, and Thomas H Heaton. epad: Earthquake probability-based automated decision-making framework for earthquake early warning. *Computer-Aided Civil and Infrastructure Engineering*, 28(10):737–752, 2013.

[51] Stephen Wu, Ming Hei Cheng, James L Beck, and Thomas H Heaton. An engineering application of earthquake early warning: epad-based decision framework for elevator control. *Journal of Structural Engineering*, page 04015092, 2015.

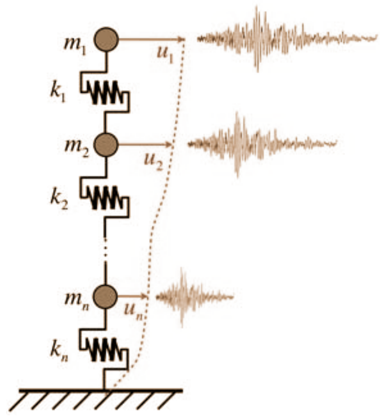

FIGURE A.1. Mass-spring system.

APPENDIX A. MODAL STIFFNESS AND MASS DERIVATIONS

A.1. **Modal Stiffness.** Consider the shear frame shown in Fig. A.1.

The stiffness matrix of subsystem i is:

$$\mathbf{k}_i = \begin{bmatrix} k_1 & -k_1 & 0 & \dots & 0 \\ -k_1 & k_1+k_2 & -k_2 & & 0 \\ 0 & -k_2 & k_2+k_3 & & \vdots \\ \vdots & \vdots & -k_3 & \ddots & -k_{i-1} \\ 0 & 0 & \cdots & & k_{i-1}+k_i \end{bmatrix} \tag{A.1}$$

with the vector of mode shape $\phi_{i,1} = \begin{Bmatrix} 1 & u_2 & u_3 & \dots & u_i \end{Bmatrix}^T$, the modal stiffness of the subsystem is:

$$k^*_{i,1} = \phi_i^T \mathbf{k}_i \phi_i = k_1 (1-u_2)^2 + k_2 (u_2-u_3)^2 + k_3 (u_3-u_4)^2 + \cdots + k_i u_i^2 \tag{A.2}$$

We eliminate the mode shape ordinates by noting that in shear frames interstory stiffnesses act as springs in series, *i.e.*:

$$k_1 (1-u_2) = k_2 (u_2-u_3) = k_3 (u_3-u_4) = \cdots = k_i u_i \tag{A.3}$$

or

$$1 - u_2 = \frac{k_i}{k_1} u_i \rightarrow u_2 = 1 - \frac{k_i}{k_1} u_i \tag{A.4}$$

$$u_2 - u_3 = \frac{k_i}{k_2} u_i \rightarrow u_3 = 1 - \frac{k_i}{k_1} u_i - \frac{k_i}{k_2} u_i = 1 - u_i \left(\frac{k_i}{k_1} + \frac{k_i}{k_2} \right) \tag{A.5}$$

$$\vdots$$

$$u_{i-1} - u_i = \frac{k_i}{k_{i-1}} u_i \rightarrow u_i \left(1 + \frac{k_i}{k_{i-1}} + \cdots + \frac{k_i}{k_2} + \frac{k_i}{k_1} \right) = 1 \tag{A.6}$$

Substituting in Eq. A.2, we have:

$$k^*_{i,1} = k_1\left(\frac{k_i}{k_1}u_i\right)^2 + k_2\left(\frac{k_i}{k_2}u_i\right)^2 + \cdots + k_i u_i^2 \tag{A.7}$$

$$= k_i u_i^2 \underbrace{\left(\frac{k_i}{k_1} + \frac{k_i}{k_2} + \cdots + \frac{k_i}{k_{i-1}} + 1\right)}_{=1/u_i} = k_i u_i \tag{A.8}$$

and with Eq. A.6,

$$k^*_{i,1} = \frac{\prod_{j=1}^{i} k_j}{\sum_{j=1}^{i}\left(\prod_{l=1,l\neq j}^{i} k_l\right)} \qquad i = 1,\ldots,n \tag{A.9}$$

which can be verified by noting that the quotient represents the equivalent stiffness of i springs in series.

A.2. **Modal Mass.** The mass matrix of subsystem i, assuming lumped masses at each floor level, is:

$$\mathbf{m}_i = \begin{bmatrix} m_1 & & & \\ & m_2 & 0 & \\ & 0 & \ddots & \\ & & & m_i \end{bmatrix} \tag{A.10}$$

and the fundamental modal mass, considering the vector of mode shape $\phi_{i,1} = \begin{Bmatrix}1 & u_2 & u_3 & \ldots & u_i\end{Bmatrix}^T$, is:

$$m^*_{i,1} = \phi^T_{i,1}\mathbf{m}_i\phi_{i,1} = m_1 + m_2u_2^2 + m_3u_3^2 + \cdots + m_iu_i^2 \tag{A.11}$$

We next present three approximations to $m^*_{i,1}$.

A.2.1. *The Dominant Term Approximation.* Note that $u_i < 1$ per (A.6) and $k_i \in \mathbb{R}^+, \forall i$. Also, $u_{i-1}^2 = 1 - 2u_i\left(\frac{k_i}{k_1} + \frac{k_i}{k_2} + \cdots + \frac{k_i}{k_{i-2}}\right) + u_i^2\left(\frac{k_i}{k_1} + \frac{k_i}{k_2} + \cdots + \frac{k_i}{k_{i-2}}\right)^2 \cong 1 - 2u_i\left(\frac{k_i}{k_1} + \frac{k_i}{k_2} + \cdots + \frac{k_i}{k_{i-2}}\right) \leq 1$ and $k_1 \leq k_2 \leq \cdots \leq k_{i-1} \leq k_i$. Therefore, as a first approximation $m^*_{i,1} \approx m_1$. Intuitively, this implies that the contribution of the top floor mass in the vibration of the fundamental mode is larger than other lower mass. With $k^*_{i,1}$ and $m^*_{i,1}$ established, the fundamental frequency of the i^{th} subsystem is

$$\omega^2_{i,1} = \frac{k^*_{i,1}}{m^*_{i,1}} \approx \widehat{\omega}^2_{1,1}\frac{\prod_{j=2}^{i} k_j}{\sum_{j=1}^{i}\left(\prod_{l=1,l\neq j}^{i} k_l\right)} \simeq \widehat{\omega}^2_{i,1} \qquad i = 1,\ldots,n \tag{A.12}$$

resulting in a set of nonlinear algebraic equations for frequencies of the subsystems that can be solved closed-form for the interstory stiffness quantities as outlined in Appendix B.

A.2.2. *The Uniform Stiffness Approximation.* To better account for the contribution of other term in (A.11) we consider the case of $k_1 = k_2 = \cdots = k_i$. With this assumption, the ordinates of the mode shape are:

$$u_2 = 1 - \frac{k_i}{k_1}u_i = 1 - u_i \tag{A.13}$$

$$u_3 = 1 - \left(\frac{k_i}{k_1} + \frac{k_i}{k_2}\right)u_i = 1 - 2u_i \tag{A.14}$$

$$\vdots$$

$$u_i = 1 - \left(\frac{k_i}{k_1} + \frac{k_i}{k_2} + \cdots + \frac{k_i}{k_{i-1}}\right)u_i = 1 - (i-1)u_i \rightarrow u_i = \frac{1}{i} \tag{A.15}$$

or, $u_2 = 1 - 1/i$, $u_3 = 1 - 2/i, \cdots, u_i = 1/i$. Hence

$$m^*_{i,1} = m_1 + m_2\left(1 - \frac{1}{i}\right)^2 + m_3\left(1 - \frac{2}{i}\right)^2 + \cdots + m_i\left(\frac{1}{i}\right)^2 \tag{A.16}$$

If $m_1 = m_2 = \cdots = m_i = m$, then

$$m^*_{i,1} = m\left[\frac{(i+1)\,(2i+1)}{6i}\right] \tag{A.17}$$

with $k^*_{i,1}$ and $m^*_{i,1}$ established, the fundamental frequency of the i^{th} subsystem is

$$\omega^2_{i,1} = \frac{k^*_{i,1}}{m^*_{i,1}} = \frac{1}{m\left[\frac{(i+1)(2i+1)}{6i}\right]}\frac{\prod_{j=1}^{i} k_j}{\sum_{j=1}^{i}\left(\prod_{l=1,l\neq j}^{i} k_l\right)} \simeq \widehat{\omega}^2_{i,1} \qquad i = 1, \ldots, n \tag{A.18}$$

resulting in a set of nonlinear algebraic equations for frequencies of the subsystems that can be solved closed-form for the interstory stiffness quantities as outlined in Appendix B.

A.2.3. *The Linear Stiffness Approximation.* We now consider the case of $k_i = \alpha k_{i-1}$, $\alpha \in \mathbb{R}^+$. Substituting in (A.13) to (A.15) we have

$$u_2 = 1 - \alpha^{i-1} u_i \tag{A.19}$$

$$u_3 = 1 - \left(\alpha^{i-2} + \alpha^{i-1}\right) u_i \tag{A.20}$$

$$\vdots$$

$$u_i = 1 - (\alpha + \alpha^2 + \cdots + \alpha^{i-1})u_i \rightarrow u_i = \frac{\alpha - 1}{\alpha^i - 1} \tag{A.21}$$

or $u_2 = \frac{\alpha^{i-1}-1}{\alpha^i-1}$, $u_3 = \frac{\alpha^{i-2}-1}{\alpha^i-1}, \cdots$, $u_i = \frac{\alpha-1}{\alpha^i-1}$. Hence for $m_1 = m_2 = \cdots = m_i = m$, we have

$$m^*_{i,1} = m\left[\left(\frac{\alpha^{i-1}-1}{\alpha^i-1}\right)^2 + \left(\frac{\alpha^{i-2}-1}{\alpha^i-1}\right)^2 + \cdots + \left(\frac{\alpha-1}{\alpha^i-1}\right)^2\right] \tag{A.22}$$

which can be further simplified by taking the first-order variation of $m^*_{i,1}$ with regards to the components of the mode shape

$$m^*_{i,1} \simeq \frac{m}{\alpha^i - 1}\left[\alpha^{i-1} + \alpha^{i-2} + \cdots + \alpha - (i-1)\right] = m\left(\frac{1}{\alpha - 1} - \frac{i}{\alpha^i - 1}\right) \tag{A.23}$$

with $k^*_{i,1}$ and $m^*_{i,1}$ established, the fundamental frequency of the i^{th} subsystem is

$$\omega^2_{i,1} = \frac{k^*_{i,1}}{m^*_{i,1}} = \frac{1}{m\left(\frac{1}{\alpha-1} - \frac{i}{\alpha^i-1}\right)}\frac{\prod_{j=1}^{i} k_j}{\sum_{j=1}^{i}\left(\prod_{l=1,l\neq j}^{i} k_l\right)} \simeq \widehat{\omega}^2_{i,1} \qquad i = 1, \ldots, n \tag{A.24}$$

resulting in a set of nonlinear algebraic equations for frequencies of the subsystems that can be solved closed-form for the interstory stiffness quantities as outlined in Appendix B.

Appendix B. Solution of the Frequency Equations

Regardless of the method of estimation of $m^*_{i,1}$ the solution of the set of equations in (A.12), (A.18), or (A.24) is available after some algebraic operations in closed-form:

(1) $i = 1$

$$\omega^2_{1,1} = \frac{k_1}{m^*_{1,1}} \simeq \widehat{\omega}^2_{1,1} \rightarrow k_1 = m^*_{1,1}\widehat{\omega}^2_{1,1} \tag{B.1}$$

(2) $i = 2$

$$\omega^2_{2,1} = \frac{k_1 k_2}{m^*_{2,1}\left(k_1 + k_2\right)} \simeq \widehat{\omega}^2_{2,1} \xrightarrow{Sub.\, k_1} k_2 = \frac{m^*_{1,1}\widehat{\omega}^2_{1,1} m^*_{2,1}\widehat{\omega}^2_{2,1}}{m^*_{1,1}\widehat{\omega}^2_{1,1} - m^*_{2,1}\widehat{\omega}^2_{2,1}} \tag{B.2}$$

(3) $i = 3$

$$\omega^2_{3,1} = \frac{k_1 k_2 k_3}{m^*_{3,1}\left(k_1 k_3 + k_2 k_3 + k_1 k_2\right)} \simeq \widehat{\omega}^2_{3,1} \xrightarrow{Sub.\, k_1\, k_2} k_3 = \frac{m^*_{2,1}\widehat{\omega}^2_{2,1} m^*_{3,1}\widehat{\omega}^2_{3,1}}{m^*_{2,1}\widehat{\omega}^2_{2,1} - m^*_{3,1}\widehat{\omega}^2_{3,1}} \tag{B.3}$$

(4) $i = n$

$$\omega^2_{n,1} = \frac{\prod_{j=1}^{n} k_j}{m^*_{n,1}\sum_{j=1}^{n}\left(\prod_{l=1,l\neq j}^{n} k_l\right)} \simeq \widehat{\omega}^2_{n,1}$$

$$\xrightarrow{Sub.\, k_1\, k_2\, \cdots\, k_{n-1}} k_n = \frac{m^*_{n-1,1}\widehat{\omega}^2_{n-1,1} m^*_{n,1}\widehat{\omega}^2_{n,1}}{m^*_{n-1,1}\widehat{\omega}^2_{n-1,1} - m^*_{n,1}\widehat{\omega}^2_{n,1}} \tag{B.4}$$

with $\frac{m^\star_{n-1,1}}{m^\star_{n,1}} > \left(\frac{\widehat{\omega}_{n,1}}{\widehat{\omega}_{n-1,1}}\right)^2$ strictly required. The identified stiffness matrix A.1 is:

$$\mathbf{k}_i = \begin{bmatrix} m^*_{1,1}\widehat{\omega}^2_{1,1} & -m^*_{1,1}\widehat{\omega}^2_{1,1} & \cdots & 0 \\ -m^*_{1,1}\widehat{\omega}^2_{1,1} & m^*_{1,1}\widehat{\omega}^2_{1,1} + \frac{m^*_{1,1}\widehat{\omega}^2_{1,1} m^*_{2,1}\widehat{\omega}^2_{2,1}}{m^*_{1,1}\widehat{\omega}^2_{1,1} - m^*_{2,1}\widehat{\omega}^2_{2,1}} & & 0 \\ 0 & -\frac{m^*_{1,1}\widehat{\omega}^2_{1,1} m^*_{2,1}\widehat{\omega}^2_{2,1}}{m^*_{1,1}\widehat{\omega}^2_{1,1} - m^*_{2,1}\widehat{\omega}^2_{2,1}} & & \vdots \\ \vdots & \vdots & \ddots & -\frac{m^*_{i-2,1}\widehat{\omega}^2_{i-2,1} m^*_{i-1,1}\widehat{\omega}^2_{i-1,1}}{m^*_{i-2,1}\widehat{\omega}^2_{i-2,1} - m^*_{i-1,1}\widehat{\omega}^2_{i-1,1}} \\ 0 & 0 & \cdots & \frac{m^*_{i-2,1}\widehat{\omega}^2_{i-2,1} m^*_{i-1,1}\widehat{\omega}^2_{i-1,1}}{m^*_{i-2,1}\widehat{\omega}^2_{i-2,1} - m^*_{i-1,1}\widehat{\omega}^2_{i-1,1}} + \frac{m^*_{i-1,1}\widehat{\omega}^2_{i-1,1} m^*_{i,1}\widehat{\omega}^2_{i,1}}{m^*_{i-1,1}\widehat{\omega}^2_{i-1,1} - m^*_{i,1}\widehat{\omega}^2_{i,1}} \end{bmatrix} \tag{B.5}$$

Identification of the stiffness matrix in this formulation is an example of parametric system identification [47].

Senior structural mechanics engineer and adjunct professor of engineering; formerly, graduate student of mathematics, Southern Methodist University

Current address: Beaverton, OR 97003

E-mail address: arzhang.alimoradi@gmail.com